Energy Equip. Sys./ Vol. 12/No. 1/March 2024/ 11-28

ENERGY EQUIPSYS

Energy Equipment and Systems

http://energyequipsys.ut.ac.ir
www.energyequipsys.com

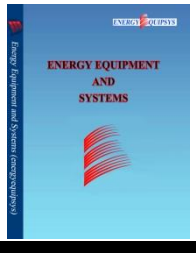

Energy harvesting from fluid flow using cantilever beam integrated with piezoelectric layer

Authors

Khalil Allah Sajadian[a]
Amirhossein Khoddami[a]
Mahbod Gholamali Sinaki[b]
Mohammad Amin Nematollahi[c]
Mohammad Hosseini[d*]

[a] Marine and Hydrokineti Energy Laboratory, School of Mechanical Engineering, College of Engineering, University of Tehran, Tehran, Iran

[b] Mechatronic Department, Department of Mechanical Engineering, Sharif University of Technology, Tehran, Iran

[c] Department of Biosystems Engineering, College of Agriculture, Shiraz University, Shiraz, Iran

[d] Department of Mechanical Engineering, Sirjan University of Technology, Sirjan, Iran

Article history:
Received : 7 July 2023
Accepted : 22 November 2023

ABSTRACT

Being inspired by nature and moving towards clean energy has become a very necessary and indispensable objective these days. By observing a collection of plants/vegetation growing underneath the rivers, oceans, and seas, the idea of designing a plant farm capable of absorb fluid energy was born. The farm comprises numerous aluminum cantilever beams equipped with a piezoelectric layer in different shapes. The field has elements of different sizes and natural frequencies, where the maximum voltage can be obtained using the resonance phenomenon. Frequency of the fluid flow is considered because it follows the oscillatory behavior of the wakes and vortices when the fluid passes through the obstacle. The Strouhal number helps to obtain the fluid frequency according to the fluid velocity and the characteristic length of the barrier. In this research, it was observed that the increase in the length of the aluminum layer caused a rise in the voltage generated. The triangular model produced a higher amount of voltage compared with the other three-dimensional models i.e. the rectangular, trapezoidal, and triangular ones. Therefore, it was concluded that providing the farm with triangular elements with different dimensions is an effective and reasonable measure. Actually, having a variety of sizes of these elements covers a wide range of natural frequencies causing a higher number of them to be excited.

Keywords: Clean Energy, Piezoelectric Layer, Fluid Energy, Fluid Frequency, Triangular Elements.

1. Introduction

Nowadays, the population growth and also the excessive utilization of fossil fuels have caused some problems such as air pollution, resources shortage, as well as the economic and environmental issues. The excessive usage of fossil fuels and, as a result, the release of pollutants and greenhouse gases could be resolved by two effective measures. One of them is to utilize renewable energy resources instead of the fossil fuels and the other one is the implementation of some energy efficiency methods in all aspects of energy production, distribution, and consumption. The point is that the energy efficiency can only reduce the fossil fuel consumption while the renewable resources can directly replace the fossil fuels [1]. Among the renewable resources, water resources specifically the ocean ones have a

* Corresponding author: Mohammad Hosseini
Department of Mechanical Engineering, Sirjan University of Technology, Sirjan, Iran
Email: hosseini@sirjantech.ac.ir

special position and have attracted a lot of attention recently. One of these energy resources is the energy harvested from the ocean tides which are available in every climate and at every moment. The two main advantages of extracting energy from these strong flows are the need for small-sized land and also the fact that it reduces some of the security concerns. The scientists believe some effective ways are needed to develop to exploit the tidal energy by the inspiration of new technologies. Additionally, it has been proved that tidal power exploitation increases the uniformity effect and helps reduce the required energy storage capacity. Also, it could enable the authorities to decrease the operating costs. A large portion of the population living in the coastal areas are the leading encouraging people to the ocean exploration for the marine energy harvest although the exploitation conditions are much harder than that on the ground[2].

The wave energy in the seas and oceans originated from the wind blowing on the water surface. Strictly speaking, the wind mechanical energy induced because of the uneven absorption of the infrared rays and visible sunlight energy is stored in sea water in the form of potential energy. Then, after a short period of time, the sea water releases the stored energy in the form of kinetic energy (wave) by the wind. The exact interaction between the wind and water surface is so complex and thus it has not been completely understood yet. It seems that the three processes of the wave development, its gradual growth and improvement are involved in this interaction [3]. Since the ocean waves energy is one of the most powerful energy resources being dissipated, use of the novel methods could harvest this energy and convert it to electricity. So far, many research have addressed the energy harvesting methods using the renewable resources found in the ocean. One of the modern ways to harvest ocean energy is to apply piezoelectric materials and install them on the marine structures. As a result of this, the piezoelectric element is deformed in interaction with the fluid and finally the strain generated in the element will induce an electric potential. The direct piezoelectricity effect is created when the element mechanical deformation causes a proportional change in the piezoelectric electrical poles. It means that when the element is loaded mechanically, the electric charge appears on the opposite side of the piezoelectric material, or on the contrary, the element deforms by the implementation of an electric voltage to it [4]. As the piezoelectric elements are usually placed against the wind or water tides in the ocean, they are subject to intensive vibrations. In a research carried out by Mutsuda et al. [5], a special model of piezoelectric whose layers had been reinforced was designed and tested numerically and experimentally in the ocean bed to investigate the electrical energy induced due to the strain applied on it. It is also feasible to extract the energy caused by the ocean waves incidence onto a piezoelectric material. Actually, the mechanical energy produced vertically when the waves break can convert the waves energy to the electrical energy. To achieve this target, a structure equipped with four piezoelectric sheet columns could be applied [6]. These columns can convert the energy exploited from the waves to the electricity in four sides. To optimize it, an optimal model for harvesting the maximum amount of strain energy while increasing the safety and life of the structure was proposed. Viet et al. [7] designed a four DOF buoyant system equipped with two piezoelectric components to harvest the ocean waves energy. This system is able to float on the sea water surface easily and produce electrical energy using the fluctuations of the sea surface. In this study, the effects of the mass, the length of the arm connected to the piezoelectric elements, the springs stiffness, as well as the waves amplitude and frequency on the output electrical energy was investigated. For this purpose, a mathematical model was derived using the Euler-Lagrange method and then after solving the obtained equations via the iteration method, the required value of electrical power was obtained. This power increases with the increase of the waves vibration amplitude, the overall mass of the system, and the piezoelectric elements young modulus and decreases when the time period of the waves vibration increases.

In similar research, the energy harvest from the ocean transversal waves using a piezoelectric plate was investigated. The

system applied for the energy exploitation was comprised of two horizontal cantilever plates connected to a rectangular column that the piezoelectric plate was attached to the free end of the cantilevers. For modeling the energy harvesting process, a mathematical model for calculating the output voltage from the piezoelectrics based on the wave theory and elastic model was defined. Then, the effects of the ocean depth, the setup location under the ocean, the plates length, the waves height, as well as the ratio of the wave's length to the ocean depth on the produced magnitude of energy was inspected. This research proposed a novel and efficient method to extract energy from the ocean utilizing piezoelectric components which was considered to be a applicable one. Xie et al. [8] studied the energy harvest from the ocean longitudinal waves analytically using a column fixed at its base and equipped with two piezoelectric layers from the both sides. In this device, the transversal oscillations cause the stimulation of the piezoelectric layers, which finally causes the electrical energy generation. Additionally, in this setup, the sea water depth measured from the bottom, the waves height and length are 3, 2, and 15 m, respectively. Nabavi et al. [9] proposed a novel way to exploit energy from the ocean waves using the piezoelectric elements mounted on the marine floaters. For this, the electromechanical equations were derived for the energy harvesting device motion exactly whose validation was verified against the experimental results. After that, the device was installed on the marine floaters. When the floaters are exposed to high-rise waves, the energy is generated in the device. The higher the waves' height, the more the produced energy. Also, the lower the frequency value created by the waves, the better the effect on the energy produced. Wu et al. [10] investigated the amount of energy could be exploited from the ocean waves applying piezoelectric floating structures. In their study, a powerful piezoelectric floating structure for electricity generation using the waves was designed. The structure consisted of several piezoelectric plates connected to a column which can be easily placed at low or high depths underneath the ocean and convert the waves' energy to the electrical one. It should be mentioned that the energy extraction procedure was carried out through the conversion of the waves transversal energy to the electricity using the piezoelectric plates connected to the floater. The findings showed that it was possible to produce up to 24 volts of electricity applying this method. Also, this device with plates and floating length of 1 and 20 m can provide the sustainable energy supply practically. In a similar research, Amini et al. [11] studied the waves energy harvesting using the piezoelectric vertical columns in horizontal fluid flows. In this study, a piezoelectric cantilever beam connected to a rotating cylinder starts to oscillate due to the vortical flow around the cylinder. Then, this oscillation causes an electrical voltage to be induced in the beam. Because the formation of the huge vortical flows leads to large amounts of mechanical energy dissipation and decreases the device efficiency as is the case in many engineering structures, piezoelectric beams, in this research, were used up for the energy harvesting whose simulations were carried out in the conditions of high and low flow velocities. The results showed that the beam undergoes intense vibrations subject to such flows and thus a significant amount of electricity could be generated accordingly. Zurkinden et al. [12] simulated a piezoelectric element and a sinusoidal wave as the model in their numerical study. In the modeling, two PVDF piezoelectric layers were used whose core was designed from foam. The selection of foam was because the designer intended the composite natural frequency to be near the value of 0.9 Hz. Jalili et al. [13]recognized utilization of the piezoelectric materials in the clean energy production as one of the appropriate methods because of the favorable influences of the mechanical-electrical coupling. In their research, a piezoelectric beam of the Euler-Bernoulli type connected to a floating cylinder and two piezoelectric layers began to vibrate through its base excitation and thus the beam could generate electricity from the induced strain energy in it. The equations of motion were derived analytically and therefore the natural frequencies could be obtained. As a result, a usable voltage could be attained assuming that the fluctuations are so small. The water flow inside a channel was

used in such a way that the wave conditions could be simulated by the vortices creation in ref. [14]. Then, a piezoelectric cantilever plate was placed in the water flow in the direction of the plate thickness and the output voltage resulting from the plate vibration was obtained. The numerical results were in a reasonable consistency with the experimental ones obtained in the smaller dimensions experimentally. It was concluded that the output voltage increased with the increase of vortices formation frequency and the decrease of the vortices distance to their formation source.

As a flow passes over an obstacle like a body, the flow pattern formed behind the body is stochastic. Therefore, the frequency of the generated flow structures like the wakes and vortices will be random accordingly. This random frequency, which is represented by a dimensionless number, known as the Strouhal number, is a function of the obstacles, especially their shapes and sizes. Actually, Strouhal number relates the flow frequency with the upcoming flow velocity and the characteristic length of the body. In our study, we introduce a novel approach to energy harvesting from fluid flow by designing a piezoelectric structure that optimally harnesses flow energy in natural environments such as seas or oceans. Our research focuses on the utilization of three-dimensional composite structures with various shapes, including triangular, rectangular, and trapezoidal elements. By creating a large farm consisting of diverse structures with varying dimensions, we aim to maximize the probability of exciting a larger number of flow structures within the farm, effectively capturing a wide range of natural frequencies. This innovative approach offers valuable insights into the design and optimization of energy harvesting systems, distinguishing our work from previous studies in the field.

2. Methodology

2.1. Geometry modeling

The structure consists of one or two PZT-5H piezoelectric layers placed on an aluminum substrate beam (Fig. 1). In three-dimensional simulations, four shapes were used for geometrical modeling including rectangular, trapezoidal (with two forms) and triangular as shown in Fig. 2. The mechanical properties of the piezoelectric material and aluminum are given in Tables 1 and 2, respectively.

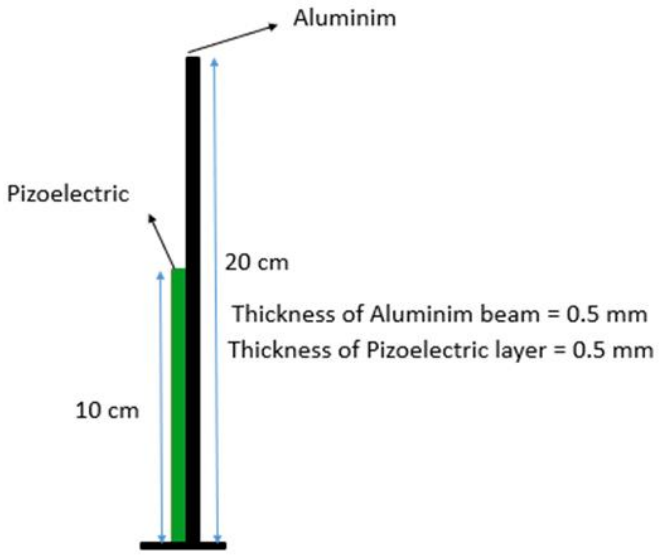

Fig. 1. Schematic of aluminum beam incorporated with a piezoelectric layer

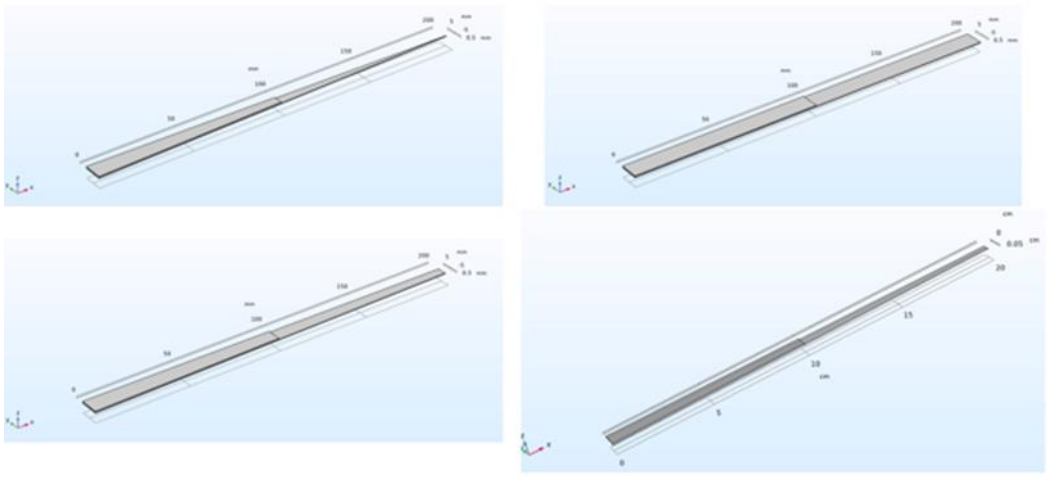

Fig. 2. Different geometries of aluminum beams equipped with piezoelectric material

Table 1. mechanical properties of the PZT-5H piezoelectric material[15]

Mechanical properties	value
Density (ρ)	7500 Kg/m^3
Young modulus (E)	4.88 GPa
Poisson ratio (v)	0.33
Charge constant (d)	274× 10^{-12} C/N
Voltage constant (g)	1.9× 10^{-3} V

Table 2. mechanical properties of Aluminium[15]

Mechanical properties	value
Density (ρ)	2700 Kg/m^3
Young modulus (E)	200 GPa
Poisson ratio (v)	0.3

The water thermophysical properties including density and dynamic viscosity are considered to be 99 kg/m^3 and $10^{-3}Pa.s$, respectively.

2.2. Computational domain and grid

The simulation is performed for the two-dimensional (2D) and the three-dimensional (3D) modeling. The 2D beam model and 3D model differ in their representation and analysis of structural behavior. In the two-dimensional beam model, the structure is simplified to a planar representation, neglecting the effects of the third dimension. This simplification assumes that the structure's cross-section remains constant along its length, and the deformations occur primarily in the plane of the structure. The governing equations for the 2D beam model typically involve simpler mathematical formulations compared to the 3D model. On the other hand, the three-dimensional model considers the full spatial dimensions of the structure. It accounts for deformations and displacements in all three directions. This allows for a more accurate representation of the structural behavior, especially when dealing with complex geometries and loadings.

The computational domain for the 2D simulations involves a two-dimensional rectangular fluid domain with the dimensions of 1.5×1 m. The domain for the 3D simulation is a rectangular cube with dimensions of 1.5×1×1 m (Fig. 3). Water enters the domain from its left side, interacts with the aluminum and piezoelectric beams and then exits the domain from the right side of it. Because of the interaction between water and the deformable beams, the physics of fluid and solid mechanics must be coupled to each other for which the fluid-structure approach (FSI) is applied. The

relevant computational domain for the three-dimensional simulations is depicted in Fig. 3.

For the grid generation of both the 2D and 3D fluid domains, triangular elements are applied. The three-dimensional computational domain is totally discretized to 392741 triangular elements. The generated 2D grids for the three mesh sizes as well as the mesh created for the 3D fluid domain are illustrated in Fig. 4 (a) and (b). As the grid study, three different 2D meshes with different sizes of elements i.e. coarse, fine, and fully fine are generated (Fig. 5) and the most reliable and suitable one is selected for the subsequent analyses. Also, several layers of boundary layer mesh are utilized for all the three meshes to observe the effects of varying the size of elements on the results obviously.

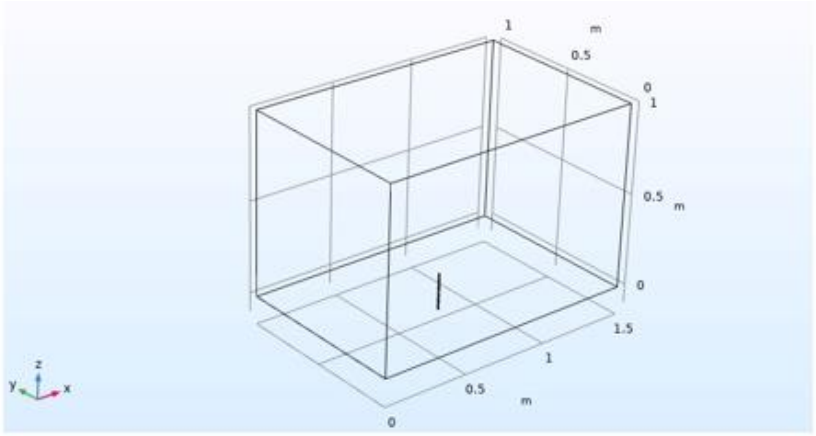

Fig. 3. Three-dimensional model of the beam in fluid domain

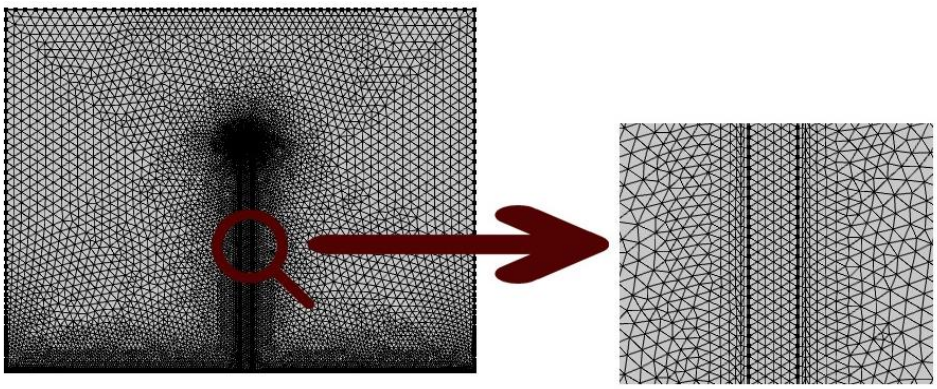

(a)

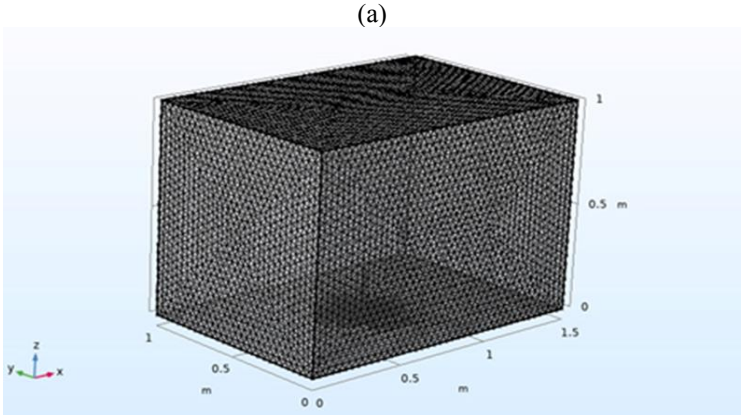

(b)

Fig. 4. Grids generated for two and three-dimensional domains. (a) 2D domain (b) 3D domain

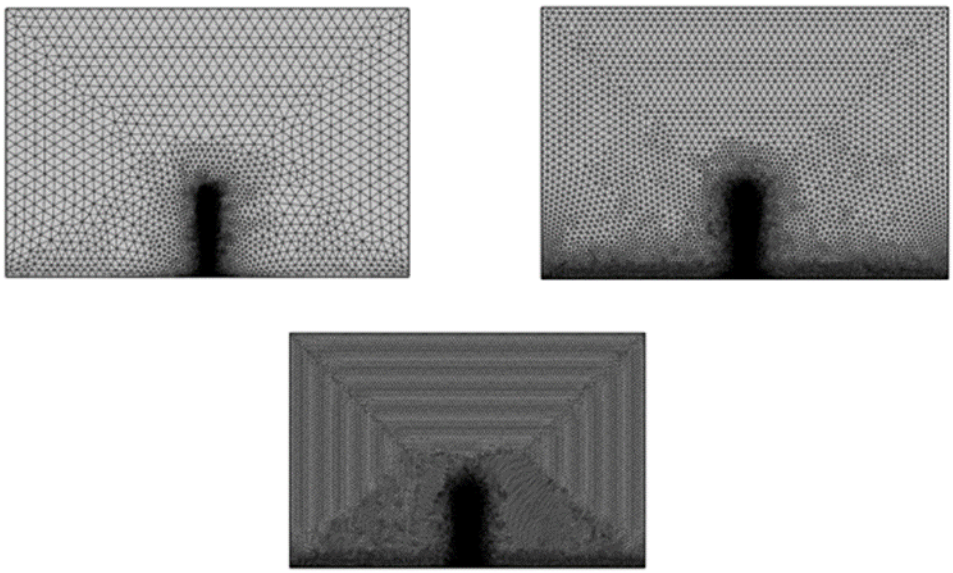

Fig. 5. Grid independency verification of the two-dimensional model of the fluid domain (upper left side fig.: 27655 elements; upper right-side fig.: 45389 elements; lower fig.: 66815 elements)

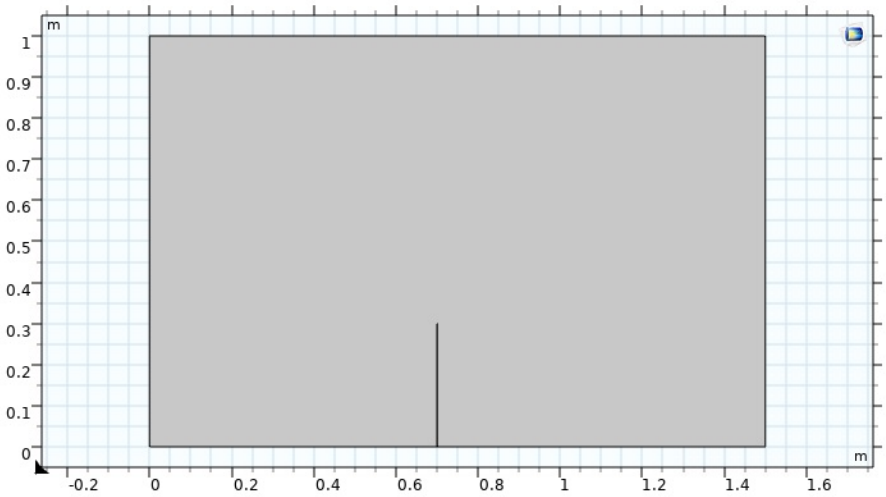

Fig. 6. Two-dimensional domain for the beam analysis

2.3. Two and three-dimensional analysis procedures

2.3.1. Two-dimensional

For two-dimensional analysis of the beam, the frequency modal analysis is performed to obtain beam's natural frequencies and also its mode shapes. After the modal analysis process, the beam is loaded in frequency space where the distributed loading is exerted on the beam by the incoming fluid. Then, the force applied by the fluid on the beam is calculated subject to different inflow velocities to the domain (Fig. 6).

Afterwards, the electrostatic and electrical circuit modules are added to the physics governing the problem to couple the mechanical stress with the electrical field. Now that these two physics have been included, the piezoelectric beam is loaded under different geometrical conditions to investigate the output voltage changes corresponding to the changes of the beam geometric specifications. These geometric changes are such that the beam length is maintained constant and the output

voltage is obtained by varying the beam thickness. In the next step, inversely, the voltage is calculated at various beam lengths while the thickness is kept at a specified value. Since the incoming flow frequencies are random, the beam loading is executed under a wide range of frequencies.

After investigating the influence of the length and thickness alteration of the piezoelectric beam on the output voltage, an aluminum cantilever is attached to the piezoelectric beam to analyze the variation of the output voltage with the increase of the aluminum beam length.

2.3.2. Three-dimensional

For three-dimensional analysis, four different geometries of the piezoelectric beam which are rectangular, trapezoidal (two different shapes), and triangular are to be analyzed to examine the effect of changing the structure geometry on the obtained voltage. The length and thickness of the beams for the simulations are chosen in such a way that they have the highest value of output voltages in the two-dimensional analyses. In our study, the thickness of both the piezoelectric and aluminum beams is equal to 0.5 mm.

2.4. Governing equations

2.4.1. Equations for fluid

Under the assumption of incompressible viscous flow, the fluid dynamics are governed by the Navier-Stokes equation as [16]:

$$\rho^F\left(\frac{\partial \boldsymbol{v}^F}{\partial t}+\boldsymbol{v}^F.\nabla\boldsymbol{v}^F\right)-\nabla.\boldsymbol{\sigma}^F=\rho^F\boldsymbol{b}^F \quad in\Omega_F \tag{1}$$

with the following continuity equations:

$$\nabla.\boldsymbol{v}^F=0 in\Omega_F \tag{2}$$

where ρ^F is the fluid density, $\boldsymbol{v}^F$ is the fluid velocity vector, $\boldsymbol{\sigma}^F$ is the fluid stress tensor, $\boldsymbol{b}^F$ is the body force vector applied to the fluid such as gravitational force, $\boldsymbol{\nabla}$ is the Nabla operator, and Ω_F is the fluid domain. A Newtonian fluid is assumed and $\boldsymbol{\sigma}^F$ is defined as follows:

$$\boldsymbol{\sigma}^F=-p\boldsymbol{I}+\mu\left(\nabla\boldsymbol{v}^F+\nabla\boldsymbol{v}^{FT}\right) \tag{3}$$

where p is the fluid pressure, $\boldsymbol{I}$ is the unit tensor, and μ is the fluid viscosity. The stress field $\boldsymbol{\sigma}^F$ is subjected to the following traction condition:

$$\boldsymbol{\sigma}^F\boldsymbol{n}^F=\boldsymbol{h}^F \tag{4}$$

where $\boldsymbol{n}^F$ is the outward normal vector and $\boldsymbol{h}^F$ is the prescribed traction.

The consideration of the gravitational force in our analysis depends on the specific conditions and assumptions made in the study. In the context of our research, we have assumed that the density of the fluid near the solid structure does not vary significantly. Under such circumstances, the influence of the gravitational force on the fluid flow can be diminished. Instead, other factors such as fluid velocity, viscosity, pressure gradients, and viscous forces become more dominant in determining the flow patterns near the solid structure. While the gravitational force is present, its impact on the flow patterns may be relatively minor compared to these other forces. Therefore, in our analysis, we have made the assumption that the gravitational force can be neglected without significantly affecting the overall understanding of the fluid flow near the vertical beam. This simplification allows us to focus on the key factors that have a more pronounced influence on the flow behavior.

Regarding the laminar flow assumption, we have considered the flow to be laminar due to the low Reynolds number associated with the external flow. The Reynolds number is a dimensionless parameter that characterizes the flow regime and is related to the ratio of inertial forces to viscous forces in the fluid. In our study, the Reynolds number for the external flow remains below the critical value of 500,000, indicating that the flow is predominantly laminar. This assumption facilitates the analysis and enables us to apply simplified mathematical models, such as the Navier-Stokes equations, to describe the fluid behavior accurately.

2.4.2. Equations for piezoelectric material and host structure

Piezoelectricity is a combination of mechanical and electrical phenomena. The mechanical

behavior is governed by the following Cauchy momentum equation:

$$\rho_0^s \frac{\partial^2 \boldsymbol{u}^s}{\partial t^2} - \nabla . \boldsymbol{\sigma}^s = \rho_0^s \boldsymbol{b}_0^s \quad in \Omega_s \tag{5}$$

where ρ_0^s is the structural density, $\boldsymbol{u}^s$ is the displacement vector, $\boldsymbol{b}_0^s$ is the body force vector, $\boldsymbol{\sigma}^s$ is the structure stress tensor and Ω_s is the domain of the solid structure. The stress field is subjected to the following traction condition:

$$\boldsymbol{\sigma}^s \boldsymbol{n}_0^s = \boldsymbol{h}_0^s \tag{6}$$

where $\boldsymbol{n}_0^s$ is the outward normal vector and $\boldsymbol{h}_0^s$ is the prescribed traction. The constitutive equations are modeled by the following linear relations:

$$\begin{aligned} \boldsymbol{\sigma}^s &= \boldsymbol{C}\,\boldsymbol{e} - \boldsymbol{d}\,\boldsymbol{E} \\ \boldsymbol{D} &= \boldsymbol{d}^T \boldsymbol{e} + \grave{o}\,\boldsymbol{E} \end{aligned} \tag{7}$$

where $\boldsymbol{e}$ is the strain tensor, $\boldsymbol{E}$ is the electric field vector, $\boldsymbol{C}$ is the elastic tensor, $\boldsymbol{d}$ is the piezoelectric tensor, and $\boldsymbol{\epsilon}$ is the dielectric tensor. The strain tensor is defined as follows:

$$\boldsymbol{e} = \frac{1}{2}\left(\nabla \boldsymbol{u}^s + \nabla \boldsymbol{u}^{sT}\right) \tag{8}$$

The piezoelectric tensor determines the degree of the coupling effect. Therefore, when $\boldsymbol{d} = \boldsymbol{0}$ holds, the mechanical response is purely governed by elasticity. By properly setting $\boldsymbol{d}$, both piezoelectric materials and elastic materials, which are used for modeling host structures, can be described.

2.4.3. Coupling conditions

Interface conditions determine how the different domains of the multi-physics system are coupled with each other, and depending on the interface conditions the modeling of the coupled domains can be either loosely coupled or strongly coupled. To complete the governing equations for the fluid-structure coupling consisting of a moving fluid-domain and vibrating elastic piezoelectric structure, coupling conditions have to be imposed on the fluid-structure interface. Geometrical continuity (or mass conservation) at the interface is achieved with the condition

$$\boldsymbol{v}^F = \frac{\partial \boldsymbol{u}^s}{\partial t} \tag{9}$$

the momentum conservation enforced on the interface is achieved using the condition given by

$$\boldsymbol{\sigma}^F \boldsymbol{n}^F + \boldsymbol{\sigma}^s \boldsymbol{n}^s = 0 \tag{10}$$

The above relation demands equal tractions along the deforming fluid-structure interface.
The steps for energy harvesting from a piezoelectric material are shown schematically in Fig. 7.

As shown in the figure, the environmental natural energy enters the piezoelectric element and then is converted to the mechanical energy in the form of mechanical vibration. Next, it changes into electrical energy under the effect of piezoelectricity.

2.5. Numerical solver and boundary conditions

For the numerical analyses involved in the problem, finite volume scheme has been applied benefiting from the finite element method (FEM) in solving the aforementioned differential equations numerically. The various physics included in the simulations are fluid flow, solid mechanics, electrostatic physics. The FEM method leads the differential equations to be converted to some sets of algebraic equations representing approximations of an unknown function on each element of the computational domain. The simple equations modeling each of these elements of the domain are then assembled into a larger set of equations containing the entire domain of the problem [17].

For the numerical simulations of the present problem, the boundary conditions are defined as follows: the velocity inlet and pressure outlet conditions are imposed to the left and right sides/surfaces of the domain, respectively. The symmetry boundary condition is implemented to the upper side/surface of the domain. For the other sides/surfaces of the domain, the no-slip wall boundary condition is defined. A schematic of the imposed boundary conditions to the different sides of the two-dimensional fluid domain is shown in Fig. 8.

Fig. 7. Schematic of energy harvesting process

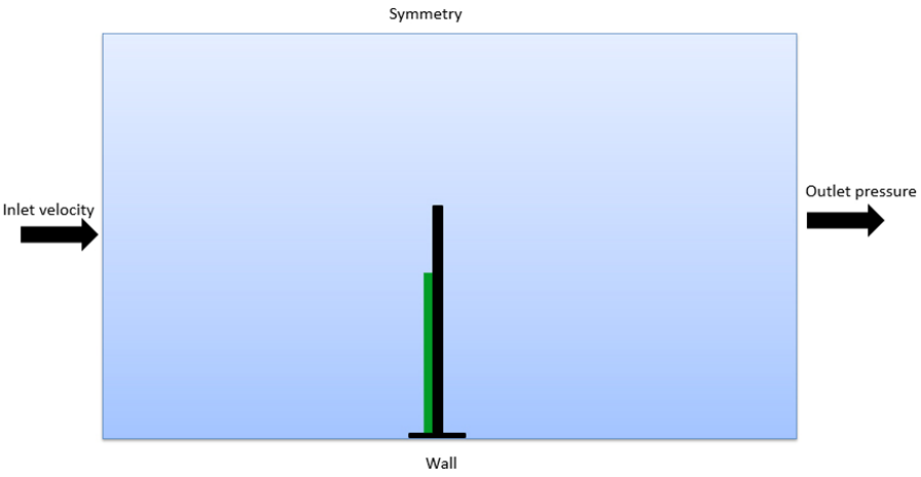

Fig. 8. Imposed boundary conditions for the computational domain

3. Results and discussion

3.1. Validation of numerical results

For the results validation, the output voltage is selected as the target parameter and then the results obtained from the numerical simulations carried out are compared with those of the Muthalif and Nordin experimental study [18]. In the experimental test, a copper cantilever beam with the specifications of 3.5 cm length, 1 cm width and 0.5 mm thickness equipped with a PZT-5H piezoelectric layer with the thickness of 0.1 mm has been loaded under a force with the magnitude of 0.2mg (where m is the overall mass of the beam and piezoelectric layer, and g denotes the acceleration of gravity) with a certain frequency range. In the numerical work, a beam with the same geometric and structural characteristics as the experimental study was simulated and then the corresponding output voltage values were recorded. The corresponding comparative output voltage versus frequency curves of both numerical and experimental studies are shown in Fig. 9. As it is evident from the curves, the variation trends of both curves are similar. In addition, the frequencies corresponding to the maximum output voltage are in the range of 250 to 300 Hz for both curves. Furthermore, the values of the maximum voltage are so close that the maximum relative error is about 8.9%. This approves a reasonable agreement between the numerical and experimental results.

The magnitudes of the hydrodynamic force exerted by the incident flow on the unit length of the cantilever beam resulted from the fluid-solid interaction (FSI) analysis have been drawn for the inflow velocities of 0.5, 1, 1.5, 3, 5, and 6 m/s values in Fig. 10.

For the analysis, the cantilever beam and the piezoelectric layer thickness are 30 cm and 0.5 mm, respectively.

According to Eq. (11) in fluid mechanics, the force exerted by a fluid on a body in the flow is proportional to the square of the fluid velocity. Meanwhile, it could be observed from Fig. 10 that a parabolic curve has been appropriately fitted to the force data and therefore it is consistent with the equation requirement.

$$F_D = 0.5 C_D \rho V^2 \tag{11}$$

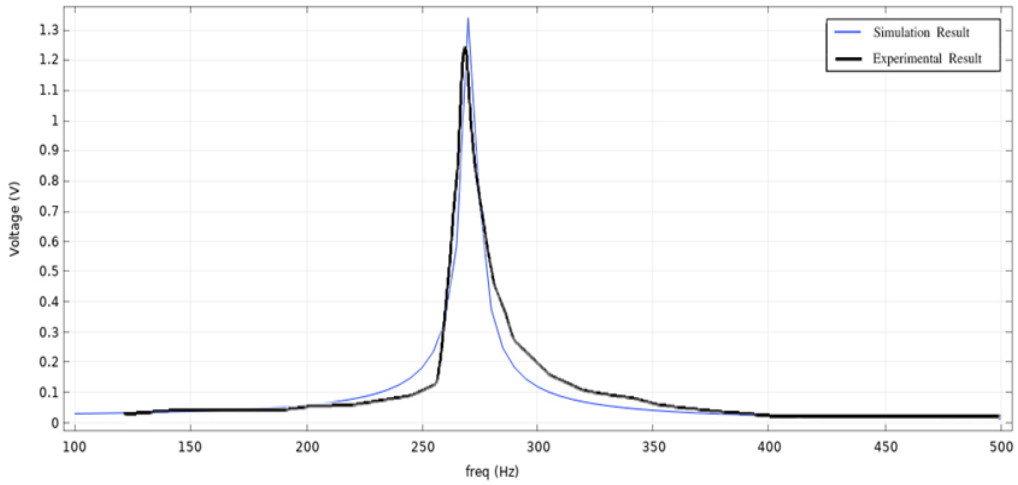

Fig. 9. Validation of the present study results against the experimental one in Ref. [18]

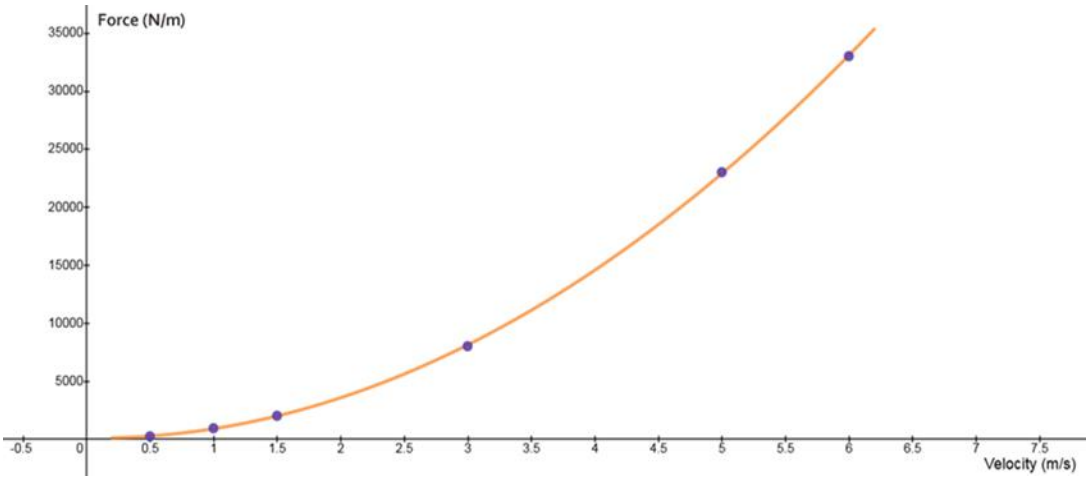

Fig. 10. The curve representing the exerted force on the beam versus inflow velocity

This finding strengthens the validation of the hydrodynamic results obtained from the fluid-solid interaction analysis. The strong agreement between the numerical and analytical data, as supported by the fitting of the parabolic curve and a high coefficient of determination (r-square), further confirms the accuracy and reliability of the hydrodynamic results. Based on this robust correlation between the numerical and analytical results, the hydrodynamic results were effectively validated through the comparison with the analytical predictions.

For more details, the contours of velocity and pressure for the velocity values of 0.5 and 3 m/s are provided in Figs. 11 and 12. These figures provide valuable insights into the flow behavior and distribution of pressures. The velocity contours offer visual representations of the flow patterns, indicating regions of high and low velocities. Similarly, the pressure contours provide information about the pressure distribution across the analyzed domain. They help in evaluating the pressure differentials and identifying regions of high and low pressures within the fluid flow.

The results of the output voltage obtained from the simulations for a piezoelectric cantilever beam with the constant thickness of 0.5 mm and the different lengths of 3.5, 5, and 10 cm at various frequencies under the condition of the inlet velocity of 2 m/s have been drawn in Fig. 13. The frequencies span a wide range of frequencies from zero to 400 Hz with 0.5 Hz frequency increment. According to the figure, it can be seen that the maximum output voltage increases with the increase of the beam length. This can be explained in this

way that the increase of the beam length leads to the more interaction of the incoming fluid with the beam and thus the greater force exerted to the beam by the fluid.

On the other hand, as the beam becomes longer, its stiffness decreases ($k = \frac{3EI}{L^3}$) and as a result, more strain is created, which induces more voltage in the beam. Also, for the same reasons mentioned above, the maximum voltage is obtained at low frequencies.

In Fig. 14 the effect of thickness variations (0.5, 1, 2, 3, and 4 mm) on the obtained voltage for a constant length (10 cm) is investigated.

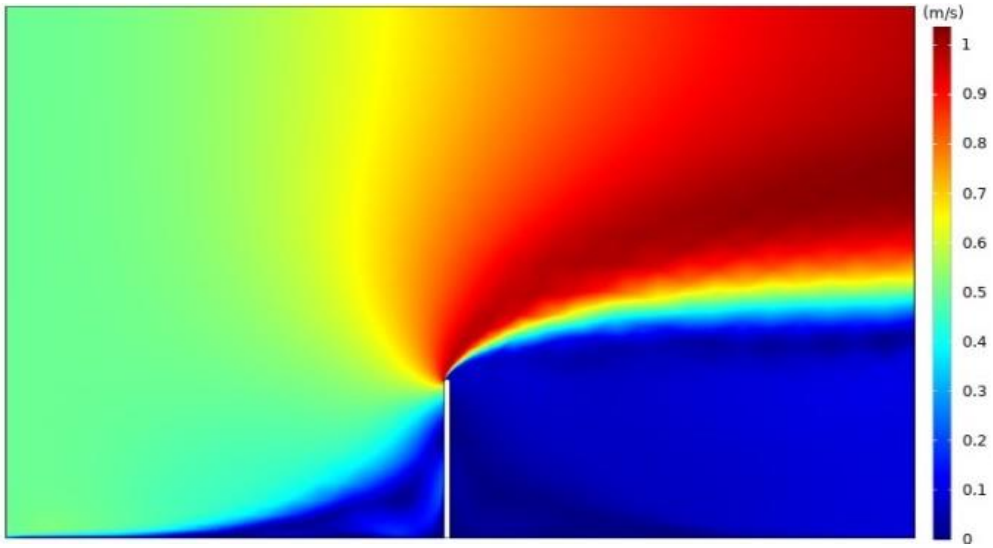

(a)

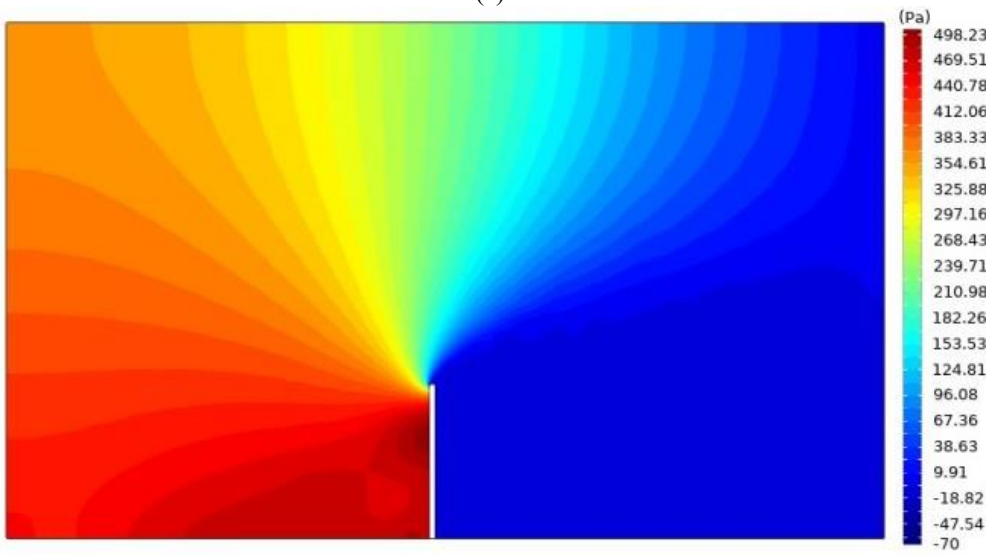

(b)

Fig. 11. (a) Velocity and (b) pressure contours at V = 0.5 m/s

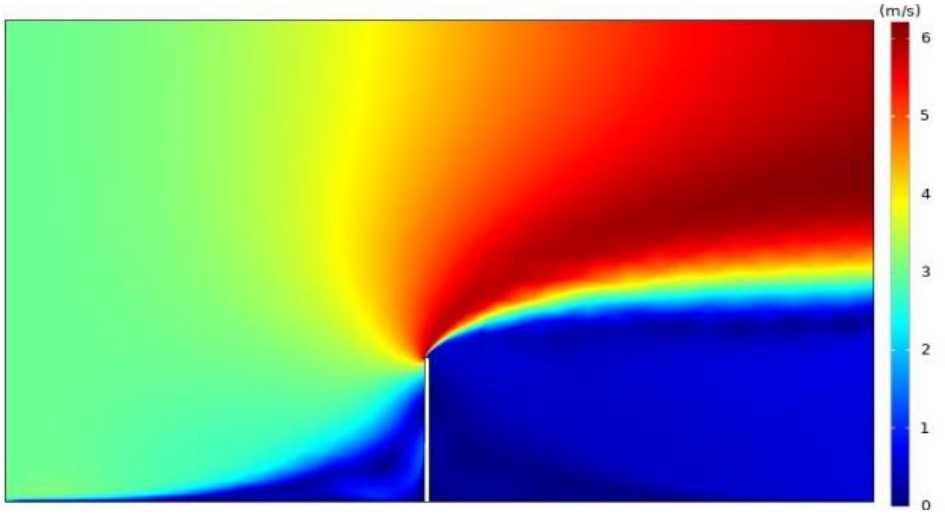

(a)

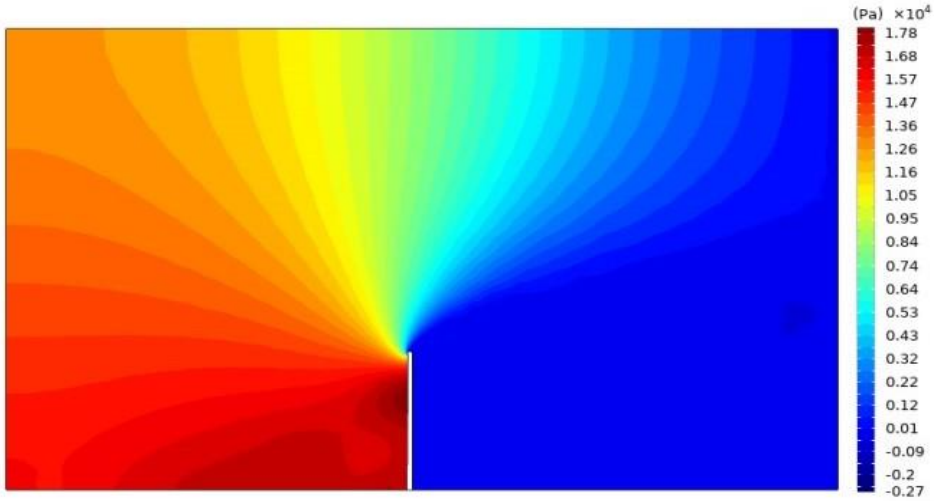

(b)

Fig. 12. (a) Velocity and (b) pressure contours at V = 3 m/s

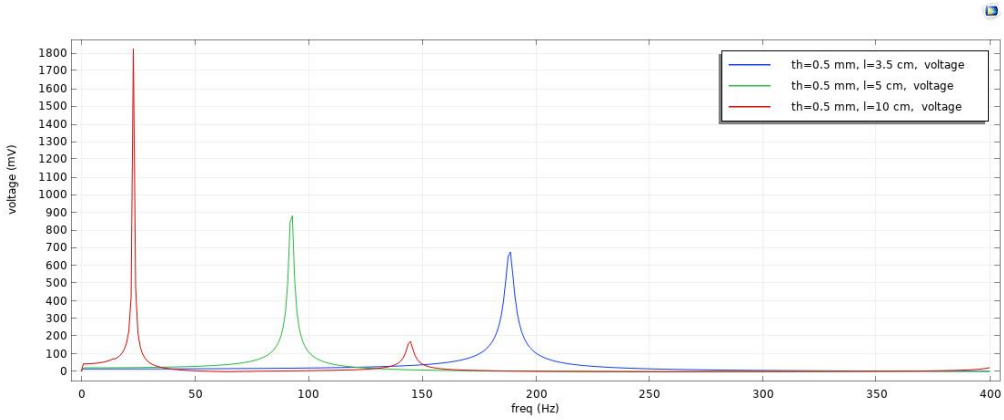

Fig. 13. Diagram of the output voltage versus frequency for different lengths of the aluminum beam

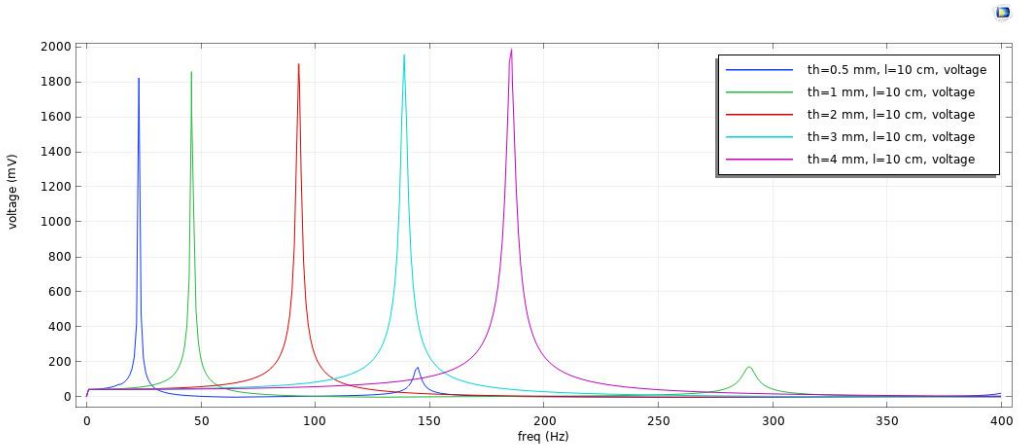

Fig. 14. Diagram of the output voltage versus frequency for different thicknesses of the piezoelectric beam

According to the figure, the results show that the induced voltage is improved by about 11% by increasing the piezoelectric thickness eight times, which is equivalent to eight times more cost.

Because of this and the fact that the piezoelectric material is so expensive, the increase of the piezoelectric thickness will not be economic and cost effective.

As it has already been shown that the output voltage increases for longer beams, aluminum beams with a piezoelectric layer are used in order to reduce the operating cost in the rest of this study, because aluminum is less expensive than piezoelectric materials. In this regard, in the continuation of the present research, the length of the aluminum beam is increased to enhance the interaction between the fluid and the beam. For this purpose, the parameter k is defined as the ratio of the beam to the initial one and varied between 1.1 and 2 ratios as shown in Fig. 15. The results of the output voltage obtained from the simulations carried out for the piezoelectric cantilever beams incorporated with a piezoelectric layer with the length and thickness of 10 cm and 0.5 mm, respectively, and the aluminum beam length values of 11, 15, and 20 cm subject to the condition 2 m/s flow inlet velocity have been depicted in Fig. 16. Additionally, the frequency magnitudes vary between zero and 100 Hz with the 0.5 Hz intervals.

From the results, as mentioned before, the longer the length of the aluminum beam, the higher induced voltage is observed. Therefore, for the next results, aluminum with k=2 is selected, which produces the highest voltage among the other investigated values. In addition, instead of one layer, it is integrated with two 10 cm piezoelectric layers with the same thickness of 0.5 mm as shown in Fig. 17.

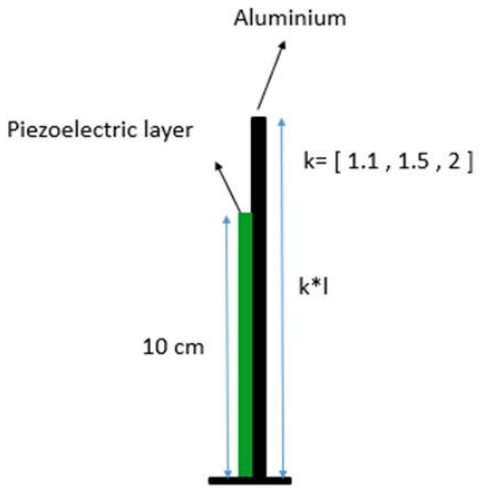

Fig. 15. parameter k changing the aluminum beam length

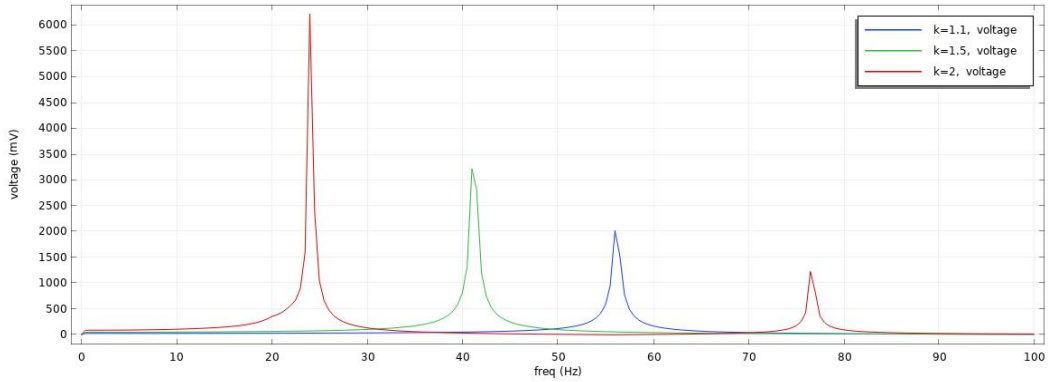

Fig. 16. Diagram of the output voltage versus frequency for different lengths of the aluminum beam incorporated with a piezoelectric layer

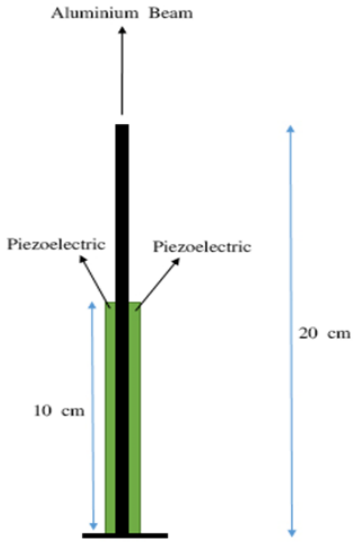

Fig. 17. Schematic of the aluminum beam equipped with two piezoelectric layers

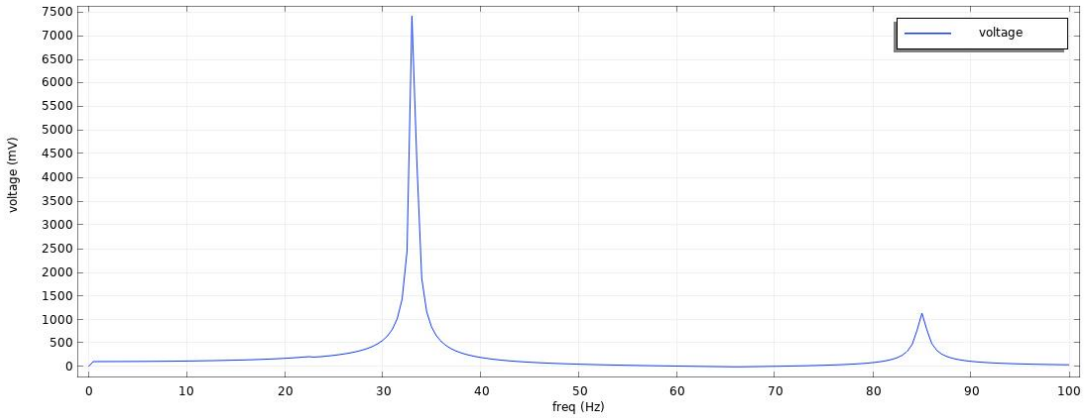

Fig. 18. Diagram of the output voltage versus frequency for the aluminum beam incorporated with two piezoelectric layers.

Figure 18 demonstrates the variation curve of the output voltage versus frequency for the case of the aluminum beam with two piezoelectric layers under the same inlet condition of the two previous results. According to the results, it is evident that despite the doubling of the operating cost with the simultaneous use of two piezoelectric layers, the output voltage does not double compared to the previous state but increases by about 15%. Therefore, although the use of two layers will increase the voltage to some extent, it will not be economical. Thus, in the following results, the aluminum beam with only one piezoelectric layer is investigated.

For the three-dimensional analysis, three different shape composites of the three-dimensional aluminum beam and piezoelectric layer were considered. According to the results, in all the four geometries, the aluminum beam and piezoelectric layer length are considered 20 and 10 cm, respectively. Furthermore, both the beam and layer thickness are equal to 0.5 mm.

For the piezoelectric layer, the width at the fixed end is 1 cm in all cases and the free end of the beam has a variable width. For this purpose, the parameter abbreviated RAT, which represents the ratio of the width of the free end of the beam to the fixed end, is introduced and varies with the values of zero, 0.2, 0.5, and 1 (Fig. 19). For this purpose, the parameter RAT, which represents the ratio of the width of the free end of the beam to the fixed end, is introduced and varies with the values of zero, 0.2, 0.5, and 1. Besides, the relevant schematic from the front view is shown in Fig. 20. The curves representing the variation of output voltage in terms of frequency for the four widths of the free end of the beam have been depicted in Fig. 21. The results were obtained from the analysis of the aluminum cantilever beam with a piezoelectric layer placed in a 2 m/s flow.

According to the curves in the above figure, the output voltage increases for the beams with the lower width at free end. This means that as the beam geometry approaches the triangular shape, the more electrical energy can be extracted.

Figure 22 illustrates the relationship between the input velocity of the fluid and the induced voltage for the optimal geometric model, specifically the three-dimensional triangular model. As the input velocity increases, the force exerted on the structure also rises. This increased force leads to a greater deflection of the structure, resulting in a corresponding increase in the induced voltage.

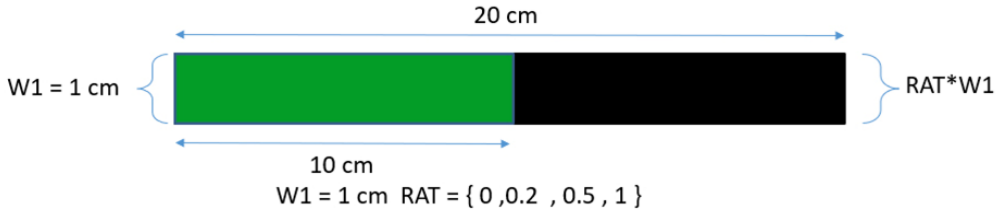

Fig. 19. Illustration of the different structure geometries with RAT ratio

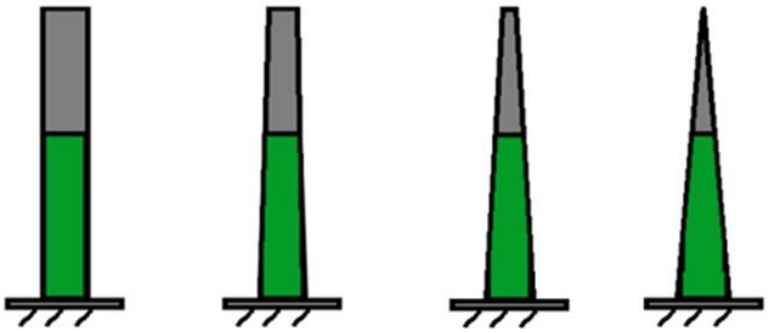

Fig. 20. Front view of the structure geometries with different values of RAT ratio

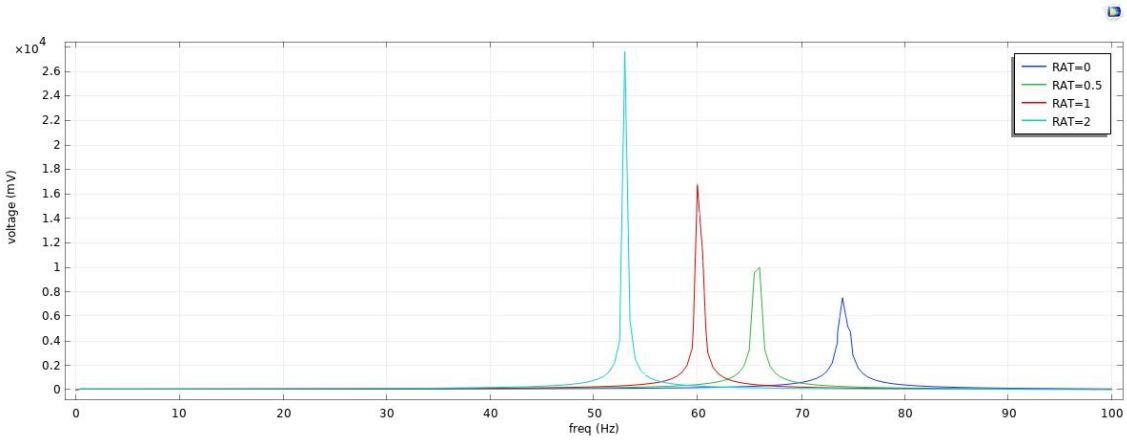

Fig. 21. Diagram of the output voltage versus frequency for four different geometries of the structure

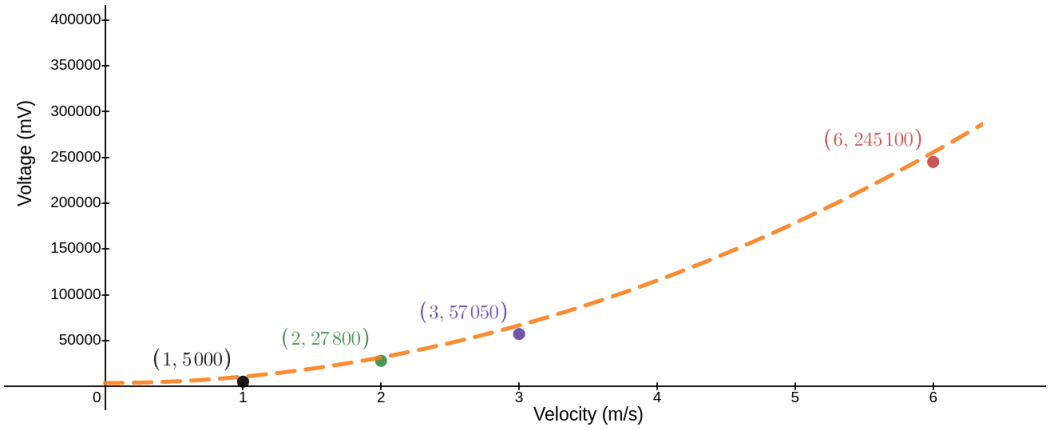

Fig. 22. Diagram representing output voltage variation against input velocity

4. Conclusion

Renewable energy resources, specially the ocean ones have a great harvest potential which can be exploited applying novel approaches. Considering this, the present work proposes an Improved geometry for an aluminum cantilever beam incorporated with a piezoelectric layer to be used in a fluid medium. This numerical study involves performing several numerical analyses to seek the structure geometry as the

Energy harvesting device. The derived model equations are based on the Euler-Bernoulli beam theory. According to the obtained results, it could be concluded that:

1. Increasing the length of both the aluminum beam and piezoelectric layer actually results in more interaction between the upstream fluid with the beams, thus causing them to receive more energy from the flow. In this way, the more load implies the more polarization of the piezoelectric material and finally the more output voltage. However, it should be noted that the beam stiffness decreases by the third power by increasing the beam length which puts the structure at risk of failure.
2. As the beam thickness increases, the output voltage rises by a small amount which is not cost-effective economically because the output voltage increases by about 15 percent if the thickness and subsequently the cost is doubled.
3. The triangular beam produces the highest output voltage value among the other geometries investigated, and since it is lighter and made of a less magnitude of piezoelectric material, it will be more cost-effective.

References

[1] J. M. C. Mehmet Kanoglu, Yunus A Cengel, Fundamentals and Applications of Renewable Energy. Mc Graw Hill, 2019.

[2] J. Courault, Marine Renewable Energy Handbook Edited by. 2012.

[3] O. U. R. Commitment, O. U. R. Strategy, E. Use, and E. Management, "Energy and Renewable Energy," pp. 2013–2014, 2014.

[4] M. Hunstig, Piezoelectric inertia motors - a critical review of history, concepts, design, appli- cations, and perspectives. 2017.

[5] H. Mutsuda, Y. Tanaka, R. Patel, Y. Doi, Y. Moriyama, and Y. Umino, "A painting type of flexible piezoelectric device for ocean energy harvesting," Appl. Ocean Res., vol. 68, pp. 182–193, 2017, doi: 10.1016/j.apor.2017.08.008.

[6] S. F. Nabavi, A. Farshidianfar, A. Afsharfard, and H. H. Khodaparast, "An ocean wave-based piezoelectric energy harvesting system using breaking wave force," Int. J. Mech. Sci., vol. 151, pp. 498–507, 2019, doi: 10.1016/j.ijmecsci.2018.12.008.

[7] N. V. Viet, X. D. Xie, K. M. Liew, N. Banthia, and Q. Wang, "Energy harvesting from ocean waves by a floating energy harvester," Energy, vol. 112, pp. 1219–1226, 2016, doi: 10.1016/j.energy.2016.07.019.

[8] X. D. Xie, Q. Wang, and N. Wu, "Energy harvesting from transverse ocean waves by a piezoelectric plate," Int. J. Eng. Sci., vol. 81, pp. 41–48, 2014, doi: 10.1016/j.ijengsci.2014.04.003.

[9] S. F. Nabavi, A. Farshidianfar, A. Afsharfard, and H. H. Khodaparast, "An ocean wave-based piezoelectric energy harvesting system using breaking wave force," Int. J. Mech. Sci., vol. 151, no. June 2018, pp. 498–507, 2019, doi: 10.1016/j.ijmecsci.2018.12.008.

[10] N. Wu, Q. Wang, and X. D. Xie, "Ocean wave energy harvesting with a piezoelectric coupled buoy structure," Appl. Ocean Res., vol. 50, pp. 110–118, 2015, doi: 10.1016/j.apor.2015.01.004.

[11] Y. Amini, M. Heshmati, P. Fatehi, and S. E. Habibi, "Piezoelectric energy harvesting from vibrations of a beam subjected to multi-moving loads," Appl. Math. Model., vol. 49, pp. 1–16, 2017, doi: 10.1016/j.apm.2017.04.043.

[12] A. S. Zurkinden, F. Campanile, and L. Martinelli, "Wave Energy Converter through Piezoelectric Polymers," 2007.

[13] P. V. Control, D6BDFCF7C799D28D8CC5854FE888C298.pdf.

[14] M. M. Hassan, M. Y. Hossain, R. Mazumder, R. Rahman, and M. A. Rahman, "Vibration energy harvesting in a small channel fluid flow using piezoelectric transducer," AIP Conf. Proc., vol. 1754, 2016, doi: 10.1063/1.4958432.

[15] L. E. Wang, Q.M., Cross, A piezoelectric pseudoshear multilayer actuator. 1998.

[16] K. Shigeki, and S. Yoshimura. "Coupled iterative partitioning analysis for flow-driven piezoelectric energy harvesters." Journal of Fluids and Structures 123 (2023): 104009.

[17] I. B. Barna Szabo, Finite Element Analysis Method, Verification, and Validation, Second Edi. Wiley Series in Computational Mechanics, 2021.

[18] A. G. A. Muthalif and N. H. D. Nordin, "Optimal piezoelectric beam shape for single and broadband vibration energy harvesting: Modeling, simulation and experimental results," Mech. Syst. Signal Process., vol. 54, pp. 417–426, 2015, doi: 10.1016/j.ymssp.2014.07.014.